PHYSICAL REVIEW D **96,** 034013 (2017)

Constructing new pseudoscalar meson nonets with the observed $X(2100)$, $X(2500)$, and $\eta(2225)$

Li-Ming Wang,[*] Si-Qiang Luo,[†] Zhi-Feng Sun,[‡] and Xiang Liu[§]

School of Physical Science and Technology, Lanzhou University, Lanzhou 730000, China
and Research Center for Hadron and CSR Physics,
Lanzhou University and Institute of Modern Physics of CAS, Lanzhou 730000, China

(Received 2 May 2017; published 16 August 2017)

Stimulated by the BESIII observation of $X(2100)$, $X(2500)$, and $\eta(2225)$, we try to pin down new pseudoscalar meson nonets including these states. The analysis of mass spectra and the study of strong decays indicate that $X(2120)$ and $\eta(2225)$ associated with $\pi(2070)$ and the predicted kaon $K(2150)$ may form a new pseudoscalar meson nonet. In addition, more experimental data for $X(2100)$ are necessary to determine its structure of nonets. Then, $X(2500)$, $X(2370)$, $\pi(2360)$, and the predicted kaon $K(2414)$ can be grouped into another new nonet. These assignments to the discussed pseudoscalar states can be further tested in experiment.

DOI: 10.1103/PhysRevD.96.034013

I. INTRODUCTION

In the pseudoscalar meson family, the first nonet is constructed by π, $\eta(548)$, $\eta'(958)$, and $K(494)$, and then the second nonet appears with the components of $\pi(1300)$, $\eta(1295)$, $\eta(1475)$, and $K(1460)$. As indicated in Ref. [1], the $X(1835)$ observed in the $\eta'\pi^+\pi^-$ invariant mass spectrum of $J/\psi \to \gamma\eta'\pi^+\pi^-$ associated with the $\eta(1760)$, $\pi(1800)$, and $K(1830)$ forms the third pseudoscalar meson nonet. By this way, one can categorize well the observed pseudoscalar states into pseudoscalar meson families. Obviously, this is not the end of the whole story.

In 2016, the BESIII Collaboration [2] performed a partial wave analysis of the $J/\psi \to \gamma\phi\phi$ decay, by which two isoscalar and pseudoscalar states $X(2100)$ (which was named as $\eta(2100)$ in Ref. [2]) and $X(2500)$ were observed with 22σ significance and 8.8σ significance, respectively. In addition, $\eta(2225)$, which was first reported in Ref. [3], was confirmed with 28σ significance. Their corresponding resonance parameters were measured as [2]

$$m_{X(2100)} = 2050^{+30+75}_{-24-26}\ \text{MeV}, \tag{1}$$

$$\Gamma_{X(2100)} = 250^{+36+181}_{-30-164}\ \text{MeV}, \tag{2}$$

$$m_{X(2500)} = 2470^{+15+101}_{-19-23}\ \text{MeV}, \tag{3}$$

$$\Gamma_{X(2500)} = 230^{+64+56}_{-35-33}\ \text{MeV}, \tag{4}$$

$$m_{\eta(2225)} = 2216^{+4+21}_{-5-11}\ \text{MeV}, \tag{5}$$

$$\Gamma_{\eta(2225)} = 185^{+12+43}_{-14-17}\ \text{MeV}. \tag{6}$$

These newly observed $X(2100)$, $X(2500)$, and $\eta(2225)$ provide us a good chance to construct new pseudoscalar meson nonets with higher radial excitations. Mainly considering this point, in this work, we study whether the newly observed $X(2100)$, $X(2500)$, and $\eta(2225)$ can be categorized into pseudoscalar meson nonets. First, we perform an analysis of the Regge trajectories, which provides an important hint of how to group these pseudoscalar states into new pseudoscalar meson families. Second, we study their two-body strong decays by the flux-tube model, which can be applied to test the possible assignments. In the following sections, we will give detailed illustrations.

When constructing pseudoscalar meson nonets with higher radial excitations, the corresponding pseudoscalar kaons are still missing in experiment. Thus, as an important theoretical prediction, the masses and decay behaviors of kaons in constructing the nonets will be given, which may provide valuable information for a future experimental search for those kaons.

This paper is organized as follows. After the Introduction, we concisely review the research status of the reported pseudoscalar states above 2 GeV in Sec. II. Then, we present a mass spectrum analysis by the approach of the Regge trajectories in Sec. III. The two-body decay behaviors of the discussed pseudoscalar states are given in Sec. IV. The paper ends with the short summary.

II. CONCISE REVIEW OF THE REPORTED PSEUDOSCALAR STATES ABOVE 2 GEV

Before the BESIII's analysis, several isoscalar and pseudoscalar states were reported [1,2,4–13], which include $\eta(2010)$, $\eta(2100)$, $\eta(2190)$, $\eta(2320)$, $X(2120)$, and $X(2370)$. However, these states are not listed in

[*]lmwang15@lzu.edu.cn
[†]luosq15@lzu.edu.cn
[‡]sunzhif09@lzu.edu.cn
[§]xiangliu@lzu.edu.cn

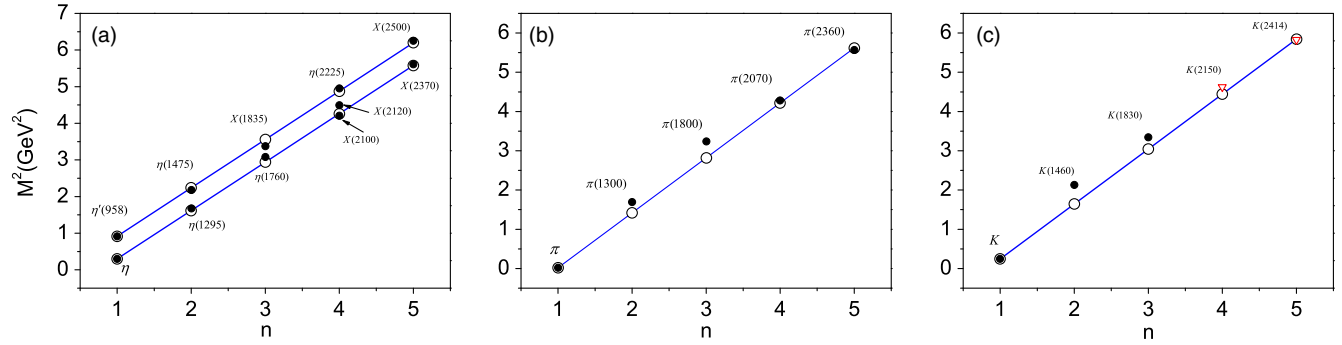

FIG. 1. The Regge trajectories for the η/η', and π and K mass spectrum with $\mu^2 = 1.32$, 1.40, and 1.40 GeV^2, respectively. Here, ∘ denotes Regge trajectories theoretical values. ▽ denotes theoretical values from Gell-Mann-Okubo mass formula [7]. And • denotes experimental values.

summary meson tables of the Particle Data Group (PDG) [14] since they are not confirmed by other experiments. It also means that these states are not established in experiment, either. The $\eta(2010)$ with mass 2010^{+35}_{-60} MeV and width 270 ± 60 MeV was found by analyzing $p\bar{p}$ annihilation into $\eta\pi^0\pi^0$, $\pi^0\pi^0$, $\eta\eta$, and $\pi^-\pi^+$ [4]. The $\eta(2100)$ was observed by the DM2 experiment in the radiative decay $J/\psi \to \gamma\rho\rho$ [5]. In Ref. [13], the $\eta(2190)$ was introduced by studying the data of the radiative decays of J/ψ into the 0^- final states [15], which has mass 2190 ± 50 MeV and width 850 ± 100 MeV. In Ref. [7], the authors discussed the possibility of the $\eta(2010)$ and $\eta(2190)$ as 4^1S_0 isoscalar states. The $\eta(2225)$ was suggested to be a good candidate for the $4^1S_0 s\bar{s}$ state [16]. The $\eta(2100)$ and $\eta(2225)$ were treated as the third radial excitations of η and η', respectively, in Ref. [7]. The $\eta(2320)$ was discovered from the combined analysis of $p\bar{p} \to \eta\eta\eta$ and $p\bar{p} \to \eta\pi\pi$ [17]. The $X(2120)$ and $X(2370)$ are two pseudoscalar states observed by BESIII in the invariant mass spectrum of the $J/\psi \to \eta'\pi^+\pi^-$ decay [6]. The observation of the $X(2120)$ and $X(2370)$ also stimulated the discussions on pseudoscalar meson, glueball, and hadronic molecular state [1,8–10]. In Ref. [9], the author has studied the mass spectrum of a baryonium with the Bethe-Salpeter equation [18–22], and $X(2370)$ can be identified as a $p\bar{N}(1400)$ bound state.

Besides the isoscalar and pseudoscalar states mentioned above, there are two isovector and pseudoscalar states $\pi(2360)$ and $\pi(2070)$ above 2 GeV, which were observed by the Crystal Barrel experiment, where the partial wave analysis of the decay $p\bar{p} \to \eta\eta\pi^0$ was done [23]. The $\pi(2360)$ has mass $M = 2360 \pm 25$ MeV and width $\Gamma = 300^{+100}_{-50}$ MeV, while the $\pi(2070)$ has mass $M = 2070 \pm 35$ MeV and width $\Gamma = 310^{+100}_{-50}$ MeV. Anisovich *et al.* suggested $\pi(2360)$ and $\pi(2070)$ as the third and fourth radial excitations of the π meson family, respectively [24]. In Ref. [7], the two-body strong decays of $\pi(2070)$ are calculated by the quark pair creation model assuming $\pi(2070)$ as $\pi(4S)$. The $\pi(2360)$ as $\pi(5^1S_0)$ was supported by the analysis of Regge trajectories [11].

From this concise review of the observed pseudoscalar states above 2 GeV, we can learn that the experimental and theoretical studies are still in chaos, especially for the isoscalar and pseudoscalar states. In the following, we try to establish new pseudoscalar meson nonets with higher radial excitations by combining the newly observed $X(2100)$, $X(2500)$, and $\eta(2225)$ with the pseudoscalar states already reported.

III. MASS SPECTRUM ANALYSIS

In the light pseudoscalar sector, η and $\eta'(958)$ together with π and K can be elements of the lowest meson nonet, while $\eta(1475), \eta(1295), K(1460)$, and $\pi(1300)$ form the meson nonet with the first radial excitation. In Refs. [1,8,9,24–26], $X(1835), \eta(1760), K(1830)$, and $\pi(1800)$ are depicted as the states with quantum number 3^1S_0. What we will discuss in this paper is the third and fourth radial excitations of pseudoscalar mesons.

The Regge trajectory analysis [27,28] is a practical way to study the mass spectrum [29–32] of mesons. The relation between mass and the radial quantum number n is

$$M^2 = M_0^2 + (n-1)\mu^2, \tag{7}$$

where M_0 and M are the masses of ground state and $(n-1)$th radial excitation state, respectively. μ^2 denotes the slope of the trajectory with the value $\mu^2 = 1.25 \pm 0.15$ GeV^2 [33].

When we plot the Regge trajectories in Fig. 1, we notice that $\pi(2070)$ and $\pi(2360)$ as well as π, $\pi(1300)$, and $\pi(1300)$ populate a common trajectory. For $\eta(4S)$, the predicted mass by the analysis of Regge trajectories is about 2064 MeV, where $\eta(2010)$, $\eta(2100)$, $\eta(2190)$, $X(2100)$, and $X(2120)$ are its candidates. Similarly, $X(2370)$, $\eta(2225)$, and $X(2500)$ are candidates for $\eta(5S)$, $\eta'(4S)$, and $\eta'(5S)$, respectively. The former theoretical studies on the masses of $\pi(4S), \eta(4S), \eta'(4S), \pi(5S)$, $\eta(5S)$, and $\eta'(5S)$ [7,11,24,33–38] are consistent with the trajectory analysis in our work.

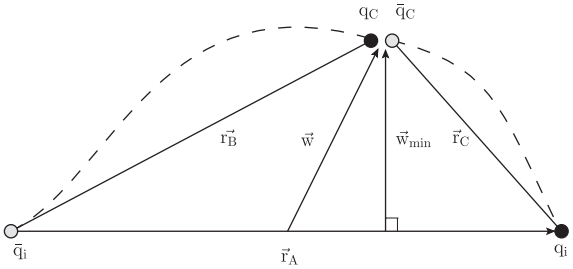

FIG. 2. The position-space coordinates used in the flux-tube model.

For the sake of completeness, the kaons with higher radial excitation should appear in the corresponding nonets. However, there is no experimental information about them with quantum numbers 4^1S_0 and 5^1S_0. With the help of diagonalization of the mass squared matrix and Gell-Mann-Okubo mass formula, the following relation is obtained [7],

$$\begin{aligned} 8X^2(M^2_{K(n^1S_0)} - M^2_{\pi(n^1S_0)})^2 &= [4M^2_{K(n^1S_0)} - (2-X^2)M^2_{\pi(n^1S_0)} - (2+X^2) \\ &\times M^2_{X(n^1S_0)}][(2-X^2)M^2_{\pi(n^1S_0)} + (2+X^2) \\ &\times M^2_{X(n^1S_0)} - 4M^2_{K(n^1S_0)}], \end{aligned} \tag{8}$$

where X describes the SU(3)-breaking ratio of the nonstrange and strange quark propagators via the constituent quark mass ratio m_u/m_s. The masses of $K(4^1S_0)$ and $K(5^1S_0)$ are predicted to be 2150 and 2414 MeV, respectively, so that we label them as $K(2150)$ and $K(2414)$, respectively. In addition, these two states are approximately located on the trajectory for kaons.

The mass information only is not sufficient to classify the structure of the states mentioned above. So, we study their two-body strong decay in the next section.

IV. TWO-BODY STRONG DECAY BEHAVIORS

A. Brief introduction of the flux-tube model

In this section, we study the strong decay behaviors of the third and fourth radial excited pseudoscalar meson nonets by the flux-tube model [12,39–43]. In the following, a brief introduction of this model is given.

The flux-tube model, first proposed by Isgur and Paton, is a useful tool for describing the decay properties of hadrons. It is suggested by the strong coupling limit of the Hamiltonian lattice QCD. In this model, a quark and an antiquark compose a meson and are connected by a chromoelectric flux tube. Here, the flux tube can be treated as a vibrating string. Figure 2 describes the picture of a meson decay, which happens when the string breaks at a point, and then the free ends of the flux tube for an initial meson (i.e., q_i and $\bar{q}_i$) connect with the quark-antiquark pair (q_C and $\bar{q}_C$) created from the vacuum.

In this paper, within the frame of the flux-tube model, the expression of a partial wave amplitude is

$$\begin{aligned} \mathcal{M}^{SL}(P) = \gamma_0 \frac{\sqrt{32\pi(2L+1)E_AE_BE_C}}{2J_A+1} \sum_{\substack{M_{L_A},M_{S_A},M_{L_B},M_{S_B},\\ M_{L_C},M_{S_C},M_{J_B},M_{J_C},m}} & \langle L0S(M_{J_B}+M_{J_C})|J_A(M_{J_B}+M_{J_C})\rangle\langle J_BM_{J_B}J_CM_{J_C}|S(M_{J_B}+M_{J_C})\rangle \\ \times \langle L_AM_{L_A}S_AM_{S_A}|J_A(M_{J_B}+M_{J_C})\rangle & \times \langle L_BM_{L_B}S_BM_{S_B}|J_BM_{J_B}\rangle\langle L_CM_{L_C}S_CM_{S_C}|J_CM_{J_C}\rangle \\ \times \langle 1m1-m|00\rangle\langle \chi^{14}_{S_BM_{S_B}}\chi^{32}_{S_CM_{S_C}}|\chi^{12}_{S_AM_{S_A}}\chi^{34}_{1-m}\rangle & \times [\langle \phi^{14}_B\phi^{32}_C|\phi^{12}_A\phi^{34}_0\rangle I^{\rm ft}(P\vec{e}_z,m_1,m_2,m_3) \\ + (-1)^{L_A+L_B+L_C+S_A+S_B+S_C}\langle \phi^{32}_B\phi^{14}_C|\phi^{12}_A\phi^{34}_0\rangle & \times I^{\rm ft}(P\vec{e}_z,m_2,m_1,m_3)]. \end{aligned} \tag{9}$$

Here, P is the momentum of a meson B. S and L denote the total spin and relative orbital angular momentum between mesons B and C, respectively. E_B is the total energy of a meson B. L_a is the orbital angular momentum between a quark and antiquark in a meson a ($a = A$, B, C). J_a is the total spin of a. M_{L_a} and M_{J_a} are the magnetic quantum numbers corresponding to L_a and J_a. m_1 and m_2 are quark masses in a meson A; m_3 is the mass of the quark and antiquark created from the vacuum. $\chi^{ij}_{s_a,m_{s_a}}$ and ϕ^{ij}_a are spin and flavor wave functions of quark i and j, and ϕ^{ij}_0 is the flavor wave function of the quark and antiquark created from the vacuum. The space integral of the last factor in Eq. (9) is given as follows,

$$\begin{aligned} I^{\rm ft}(P\vec{e}_z,m_1,m_2,m_3) &= -\frac{8}{(2\pi)^{3/2}}\int d^3\vec{r}\int d^3\vec{w} \\ &\times \psi^*_{n_BL_BM_{L_B}}(-\vec{w}-\vec{r})\psi^*_{n_CL_CM_{L_C}}(\vec{w}-\vec{r}) \\ &\times y^m_1([(P\vec{e}_z + i\vec{\nabla}_{\vec{r}_A})\psi_{n_AL_AM_{L_A}}(\vec{r}_A)]_{\vec{r}_A=-2\vec{r}}) \\ &\times \exp\left(-\frac{1}{2}bw^2_{\rm min}\right)\exp(i\vec{P}\cdot(m_+\vec{r}+m_-\vec{w})), \end{aligned} \tag{10}$$

with $m_+ = \frac{m_1}{m_1+m_3} + \frac{m_2}{m_2+m_3}$, $m_- = \frac{m_1}{m_1+m_3} - \frac{m_2}{m_2+m_3}$. The quark pair creation (QPC) model [15] was first proposed by Micu to calculate Okubo-Zweig-Iizuka (OZI) strong decays. In the QPC model, the heavy flavor meson decay

TABLE I. The partial decay widths measured for ten decay channels and the comparison with theoretical calculations.

Decay channel	Experiment (MeV) [14]	Our fit (MeV)
$\rho \to \pi\pi$	147.8	83.3
$b_1(1235) \to \omega\pi$	142	129.5
$f_2(1270) \to \pi\pi$	156.5	85.1
$f_2' \to K\bar{K}$	64.8	90.6
$K^* \to K\pi$	50.8	34.9
$K_0^*(1430) \to K\pi$	251	381.3
$K_2^*(1430) \to K\pi$	49.1	63.9
$K_2^*(1430) \to K^*\pi$	24.3	33.8
$K_3^*(1780) \to K^*\pi$	49.3	42.6
$K_3^*(1780) \to K\pi$	28.6	46.5

occurs through a quark-antiquark pair production from the vacuum, which has the quantum number of the vacuum, i.e., 0^{++}. In the QPC model, the constant γ is used to depict the strength of the quark pair creation from the vacuum. However, in the flux-tube model, γ is not a constant and is given by [44]

$$\gamma(\bar{r}, \bar{w}) = \gamma_0 e^{-\frac{1}{2}bw_{\min}^2}. \quad (11)$$

In Eq. (9), γ_0 is a new phenomenological parameter, which can be fixed as 14.8 by fitting the experimental data from the PDG (see Table I). b is the string tension which has the typical value 0.18 GeV^2, and $w_{\min}$ is the shortest distance

TABLE II. The allowed two-body decays of $X(2100), \eta(2225), X(2370), X(2500), \pi(2070)$, and $\pi(2360)$ are marked by $\surd$. Here, ρ, ϕ, and ω denote $\rho(770), \phi(1020)$, and $\omega(782)$, respectively.

Modes	Channel	$X(2100)$	$\eta(2225)$	$X(2370)$	$X(2500)$	Channel	$\pi(2070)$	$\pi(2360)$
$0^- + 0^+$	$\pi a_0(980)$	$\surd$	$\surd$	$\surd$	$\surd$	$\eta a_0(980)$	$\surd$	$\surd$
	$\pi a_0(1450)$	$\surd$	$\surd$	$\surd$	$\surd$	$\eta a_0(1450)$	$\surd$	$\surd$
	$\pi(1300)a_0(980)$			$\surd$	$\surd$	$\eta' a_0(980)$	$\surd$	$\surd$
	$KK_0^*(1430)$	$\surd$	$\surd$	$\surd$	$\surd$	$\eta(1295)a_0(980)$		$\surd$
						$KK_0^*(1430)$	$\surd$	$\surd$
$1^- + 1^+$	$\rho b_1(1235)$	$\surd$	$\surd$	$\surd$	$\surd$	$\rho(770)h_1(1170)$	$\surd$	$\surd$
	$\omega h_1(1170)$	$\surd$	$\surd$	$\surd$	$\surd$	$\rho(770)h_1(1380)$		$\surd$
	$\phi h_1(1170)$		$\surd$	$\surd$	$\surd$	$\omega(782)b_1(1235)$	$\surd$	$\surd$
	$\phi h_1(1380)$				$\surd$	$K^*K_1(1270)$		$\surd$
	$K^*K_1(1270)$			$\surd$	$\surd$	$K^*K_1(1400)$		$\surd$
	$K^*K_1(1400)$			$\surd$	$\surd$	$\rho(770)a_1(1260)$	$\surd$	$\surd$
$0^- + 1^-$	$KK^*(1410)$	$\surd$	$\surd$	$\surd$	$\surd$	KK^*	$\surd$	$\surd$
	KK^*	$\surd$	$\surd$	$\surd$	$\surd$	$KK^*(1410)$	$\surd$	$\surd$
	$KK^*(1680)$		$\surd$	$\surd$	$\surd$	$KK^*(1680)$		$\surd$
	$K(1460)K^*$			$\surd$	$\surd$	$K(1460)K^*$		$\surd$
						$\pi\rho(770)$	$\surd$	$\surd$
						$\pi\rho(1450)$	$\surd$	$\surd$
						$\pi\rho(1700)$	$\surd$	$\surd$
						$\pi(1300)\rho(770)$		$\surd$
$0^+ + 1^+$	$a_0(980)a_1(1260)$			$\surd$	$\surd$	$a_0(980)f_1(1285)$		$\surd$
						$a_0(980)b_1(1235)$		$\surd$
$1^- + 1^-$	$\rho\rho$	$\surd$	$\surd$	$\surd$	$\surd$	$\rho(770)\omega(782)$	$\surd$	$\surd$
	$\rho\rho(1450)$		$\surd$	$\surd$	$\surd$	$\rho(770)\omega(1420)$	$\surd$	$\surd$
	$\omega\omega$	$\surd$	$\surd$	$\surd$	$\surd$	$\omega(782)\rho(1450)$		$\surd$
	$\omega\omega(1420)$		$\surd$	$\surd$	$\surd$	K^*K^*	$\surd$	$\surd$
	$\phi\phi$	$\surd$	$\surd$	$\surd$	$\surd$	$K^*K^*(1410)$		$\surd$
	K^*K^*	$\surd$	$\surd$	$\surd$	$\surd$			
	$K^*K^*(1410)$			$\surd$	$\surd$			
$0^- + 2^+$	$\pi a_2(1320)$	$\surd$	$\surd$	$\surd$	$\surd$	$\pi f_2(1270)$	$\surd$	$\surd$
	$\pi a_2(1700)$	$\surd$	$\surd$	$\surd$	$\surd$	$\eta a_2(1320)$	$\surd$	$\surd$
	$\eta f_2(1270)$	$\surd$	$\surd$	$\surd$	$\surd$	$\eta a_2(1700)$		$\surd$
	$\eta f_2'(1270)$		$\surd$	$\surd$	$\surd$	$\eta' a_2(1320)$		$\surd$
	$\eta' f_2(1270)$			$\surd$	$\surd$	$KK_2^*(1430)$	$\surd$	$\surd$
	$KK_2^*(1430)$	$\surd$	$\surd$	$\surd$	$\surd$			
$1^- + 2^+$	$K^*K_2^*(1430)$			$\surd$	$\surd$	$K^*K_2^*(1430)$		$\surd$
						$\rho(770)a_2(1320)$		$\surd$
$0^- + 3^-$	$KK_3^*(1780)$			$\surd$	$\surd$	$KK_3^*(1780)$		$\surd$
$0^- + 4^+$	$\pi a_4(2030)$		$\surd$	$\surd$	$\surd$			

TABLE III. The allowed two-body decays of $K(2150)$ and $K(2414)$ are marked by $\surd$. Here, ρ, ϕ, and ω denote $\rho(770)$, $\phi(1020)$, and $\omega(782)$, respectively.

Channel	$K(2150)$	$K(2414)$	Channel	$K(2150)$	$K(2414)$
$\pi K_0^*(1430)$	$\surd$	$\surd$	$\eta K_0^*(1430)$	$\surd$	$\surd$
$\eta^* K_0^*(1430)$		$\surd$	$Ka_0(980)$	$\surd$	$\surd$
$Ka_0(1450)$		$\surd$	$\rho K_1(1270)$	$\surd$	$\surd$
$\rho K_1(1400)$		$\surd$	$\omega K_1(1270)$	$\surd$	$\surd$
$\omega K_1(1400)$		$\surd$	$\phi K_1(1270)$		$\surd$
$K^* h_1(1170)$	$\surd$	$\surd$	$K^* h_1(1380)$		$\surd$
$K^* b_1(1235)$	$\surd$	$\surd$	$K^* a_1(1260)$		$\surd$
$K^* f_1(1285)$		$\surd$	$K^* f_1(1420)$		$\surd$
πK^*	$\surd$	$\surd$	$\pi K^*(1410)$	$\surd$	$\surd$
$\pi K^*(1680)$		$\surd$	ηK^*	$\surd$	$\surd$
$\eta K^*(1410)$	$\surd$	$\surd$	$\eta K^*(1680)$		$\surd$
$\eta' K^*$	$\surd$	$\surd$	$\eta' K^*(1410)$	$\surd$	$\surd$
$\pi(1300) K^*$		$\surd$	$K\rho$	$\surd$	$\surd$
$K\omega$	$\surd$	$\surd$	$K\phi$	$\surd$	$\surd$
$K\omega(1420)$	$\surd$	$\surd$	$K\rho(1450)$	$\surd$	$\surd$
$K\omega(1650)$	$\surd$	$\surd$	$K\phi(1680)$		$\surd$
$K(1460)\rho$		$\surd$	$K(1460)\omega$		$\surd$
$a_0(980) K_1(1270)$		$\surd$	$a_0(980) K_1(1400)$		$\surd$
ρK^*	$\surd$	$\surd$	$\rho K^*(1410)$		$\surd$
ωK^*	$\surd$	$\surd$	$\omega K^*(1410)$		$\surd$
ϕK^*	$\surd$	$\surd$	$\rho(1450) K^*$		$\surd$
$\omega(1420) K^*$		$\surd$	$K f_2(1270)$	$\surd$	$\surd$
$Ka_2(1320)$	$\surd$	$\surd$	$K f_2'(1525)$	$\surd$	$\surd$
$Ka_2(1700)$		$\surd$	$\pi K_2^*(1430)$	$\surd$	$\surd$
$\eta K_2^*(1430)$	$\surd$	$\surd$	$\eta' K_2^*(1430)$		$\surd$
$K^* f_2(1270)$		$\surd$	$K^* a_2(1320)$		$\surd$
$\omega K_2^*(1430)$		$\surd$	$\rho K_2^*(1430)$		$\surd$
$\pi K_3^*(1680)$		$\surd$	$\eta K_3^*(1680)$		$\surd$

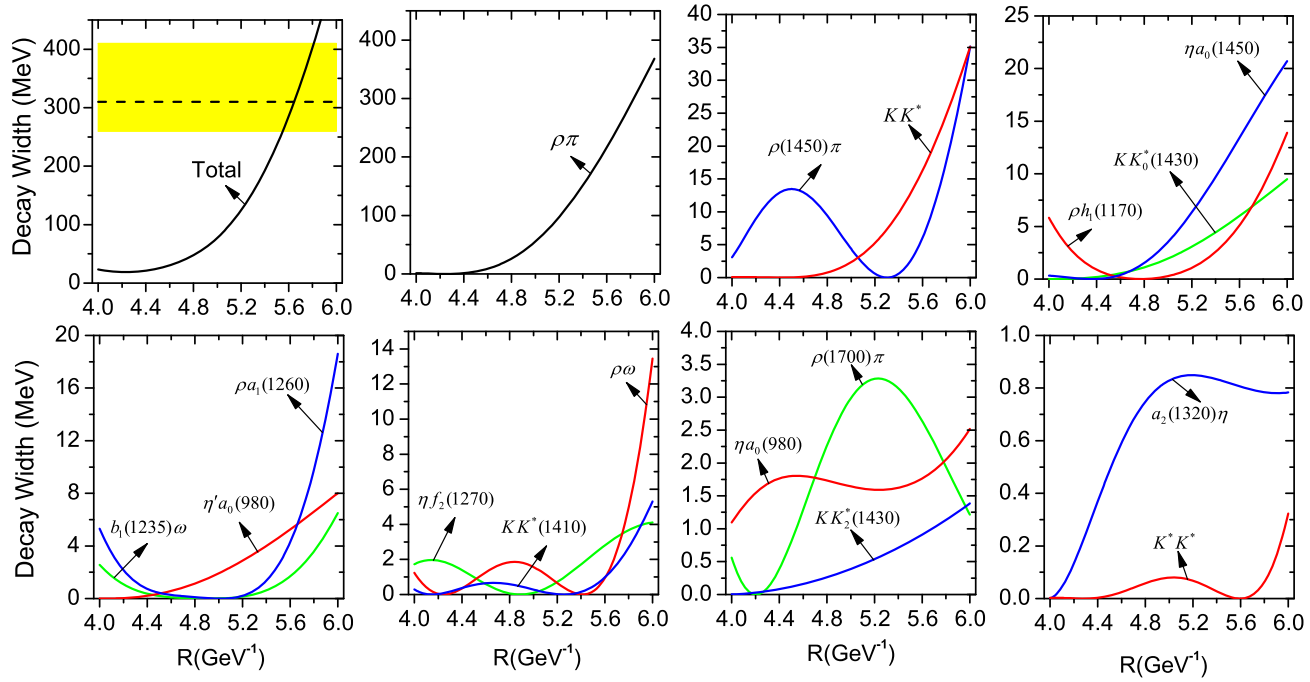

FIG. 3. The R dependence of two-body strong decay widths of $\pi(2070)$ as a $\pi(4S)$ state. The experimental data are marked by the yellow band. Some tiny channels are not drawn.

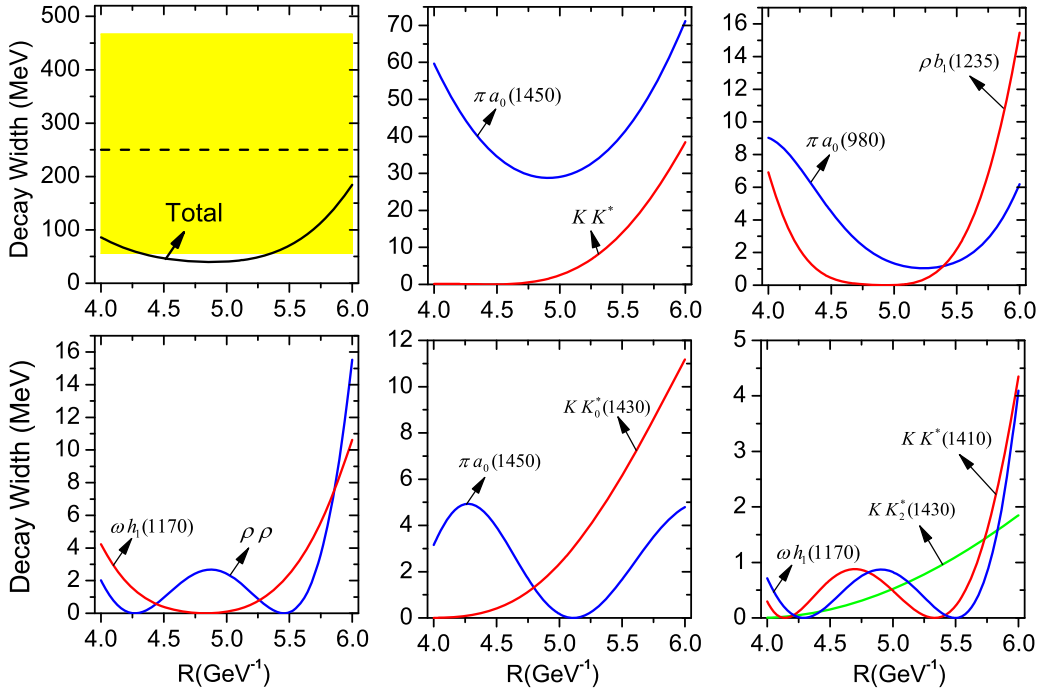

FIG. 4. The R dependence of the total decay width and partial two-body decay widths of $X(2100)$ as the third radial excitation of η. The experimental data are marked by the yellow band. Some tiny channels are not drawn. Here, the mixing angle we take is $-2.61°$.

between the points, where the quark-antiquark pair is created from the vacuum to the segment connecting the original quark and antiquark in an initial state (see Fig. 2). The expression of $w^2_{\rm min}$ reads

$$w^2_{\rm min} = \begin{cases} w^2\sin^2\theta & \text{if } r \geq w|\cos\theta| \\ r^2 + w^2 - 2rw|\cos\theta| & \text{if } r < w|\cos\theta| \end{cases}. \quad (12)$$

Then, one can get the decay width

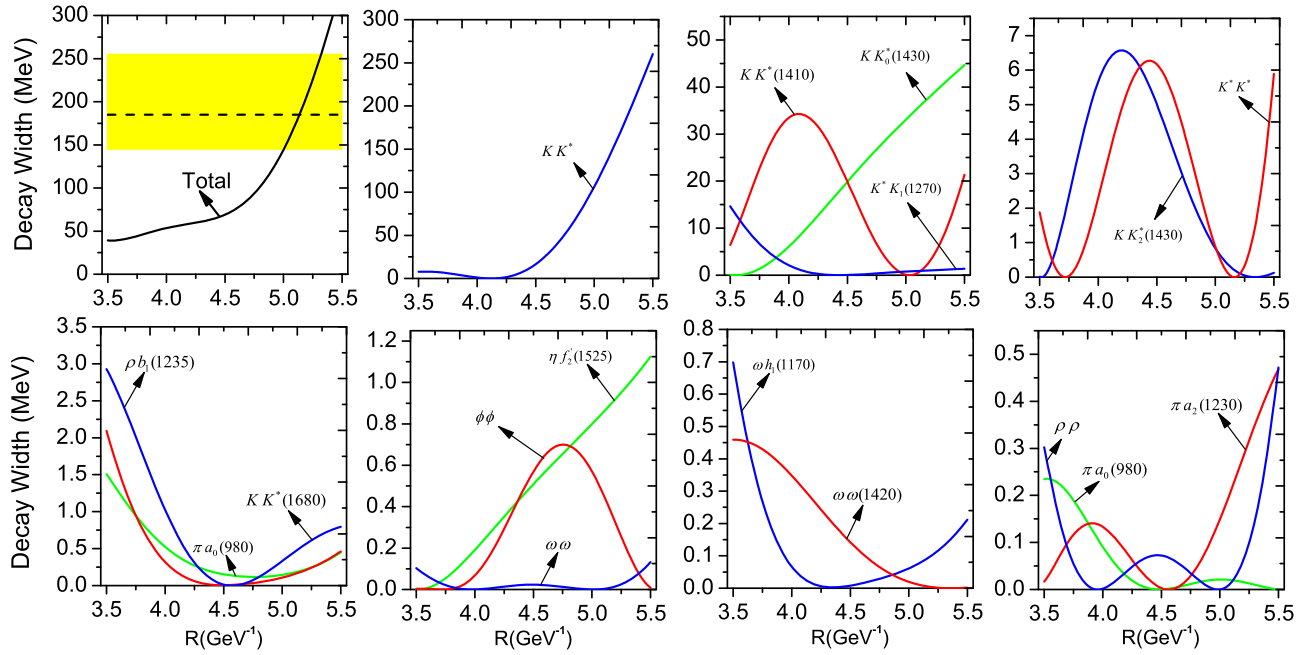

FIG. 5. The R dependence of total decay width and partial two-body decay widths of $\eta(2225)$ as the third radial excitation of η. The experimental data are marked by the yellow band. Some tiny channels are not drawn. Here, the mixing angle we take is $6.93°$.

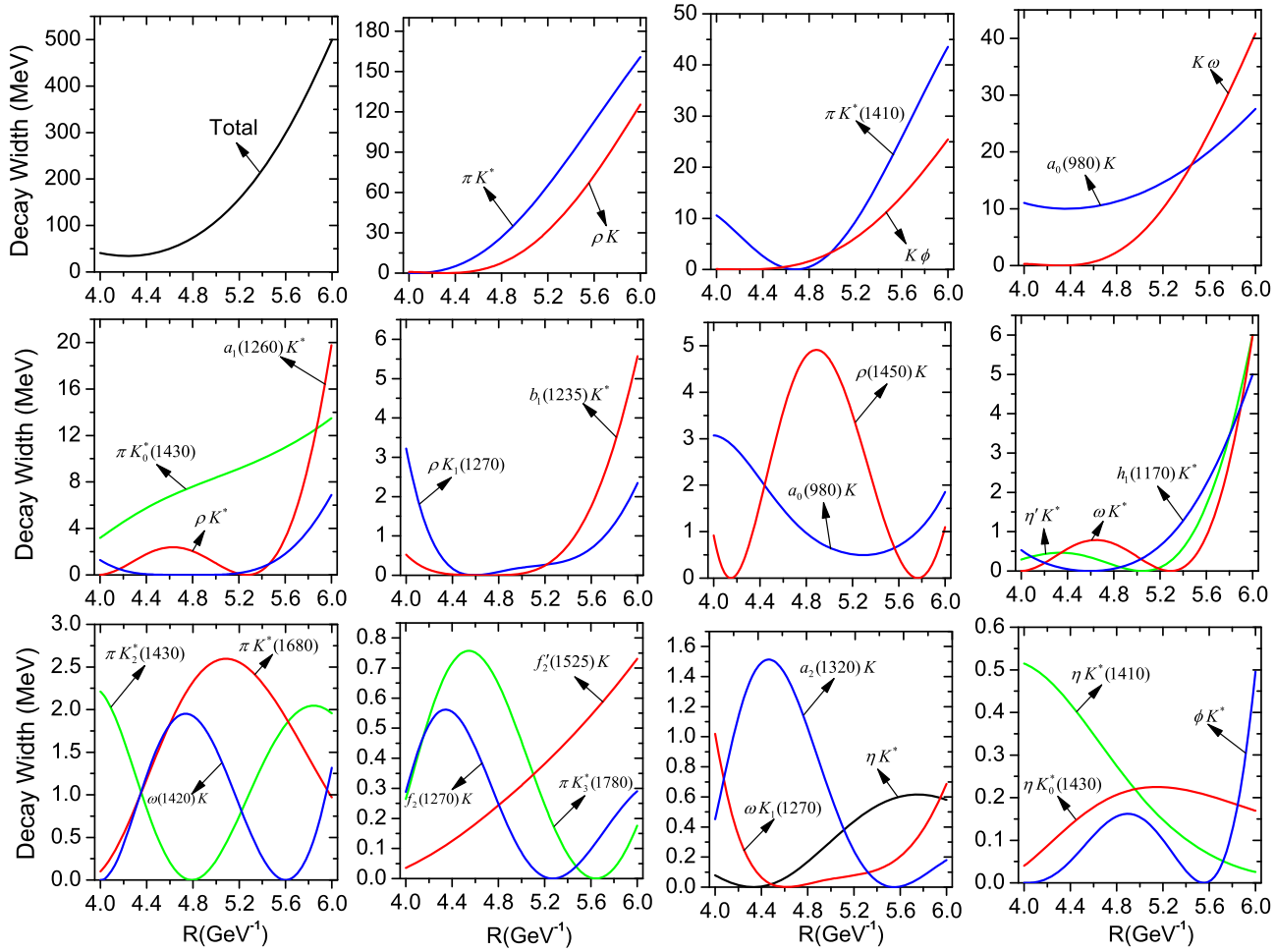

FIG. 6. The R dependence of two-body decay widths of $K(2150)$ as the third radial excitation of K. Some tiny channels are not drawn.

$$\Gamma = \frac{\pi}{4}\frac{|\mathbf{P}|}{M_A^2}\sum_{LS}|\mathcal{M}^{LS}|^2. \tag{13}$$

In order to simplify the calculation, we use the simple harmonic oscillator (SHO) wave function to depict the meson, which reads

$$\psi_{nLM_L}(\mathbf{r}) = R_{nL}^{\mathrm{SHO}}(r)Y_{LM_L}(\mathbf{\Omega}_r) \tag{14}$$

with the radial wave function

$$R_{nL}^{\mathrm{SHO}}(r) = \frac{1}{R^{3/2}}\sqrt{\frac{2n!}{\Gamma(n+L+3/2)}}(r/R)^L \times e^{-\frac{r^2}{2R^2}}L_n^{L+1/2}(r^2/R^2). \tag{15}$$

Here, $L_n^{L+1/2}(r^2/R^2)$ is an associated Laguerre polynomial. The parameter R is determined by reproducing the realistic root mean square radius by solving the Schrödinger equation with the linear potential plus color Coulomb and Gaussian-smeared contact hyperfine term [45]. The R value can be obtained through the relation [46,47]

$$\int |\psi_{nLM_L}^{\mathrm{SHO}}(\mathbf{r})|^2 r^2 d^3\mathbf{r} = \int |\Phi(\mathbf{r})|^2 r^2 d^3\mathbf{r}. \tag{16}$$

The $\Phi(\mathbf{r})$ is the wave function of a certain meson in the potential model [48].

B. Fourth pseudoscalar meson nonet

As discussed in Sec. III, $\eta(2010)$, $\eta(2100)$, $X(2120)$, and $\eta(2190)$ can be regarded as the candidates of the third radial excitation of $\eta(548)$, while $\eta(2225)$ is the candidate of $\eta'(4S)$. Besides, $\pi(2070)$ can be a 4^1S_0 state. We also analyze the mass of the third radial excitation of the kaon, which is around 2151 MeV and labeled as $K(2150)$ here. In Tables II and III, the decay channels are listed. In the following, we present the strong decay properties of these particles.

In Fig. 3, we show the total and partial decay widths of $\pi(2070)$ as a 4^1S_0 state. By comparing our theoretical results with the experimental data, the R value lies in the range $5.55 \sim 5.81$ GeV^{-1}, which is consistent with that in Ref. [24]. $\rho\pi$ is the dominant decay channel with the width

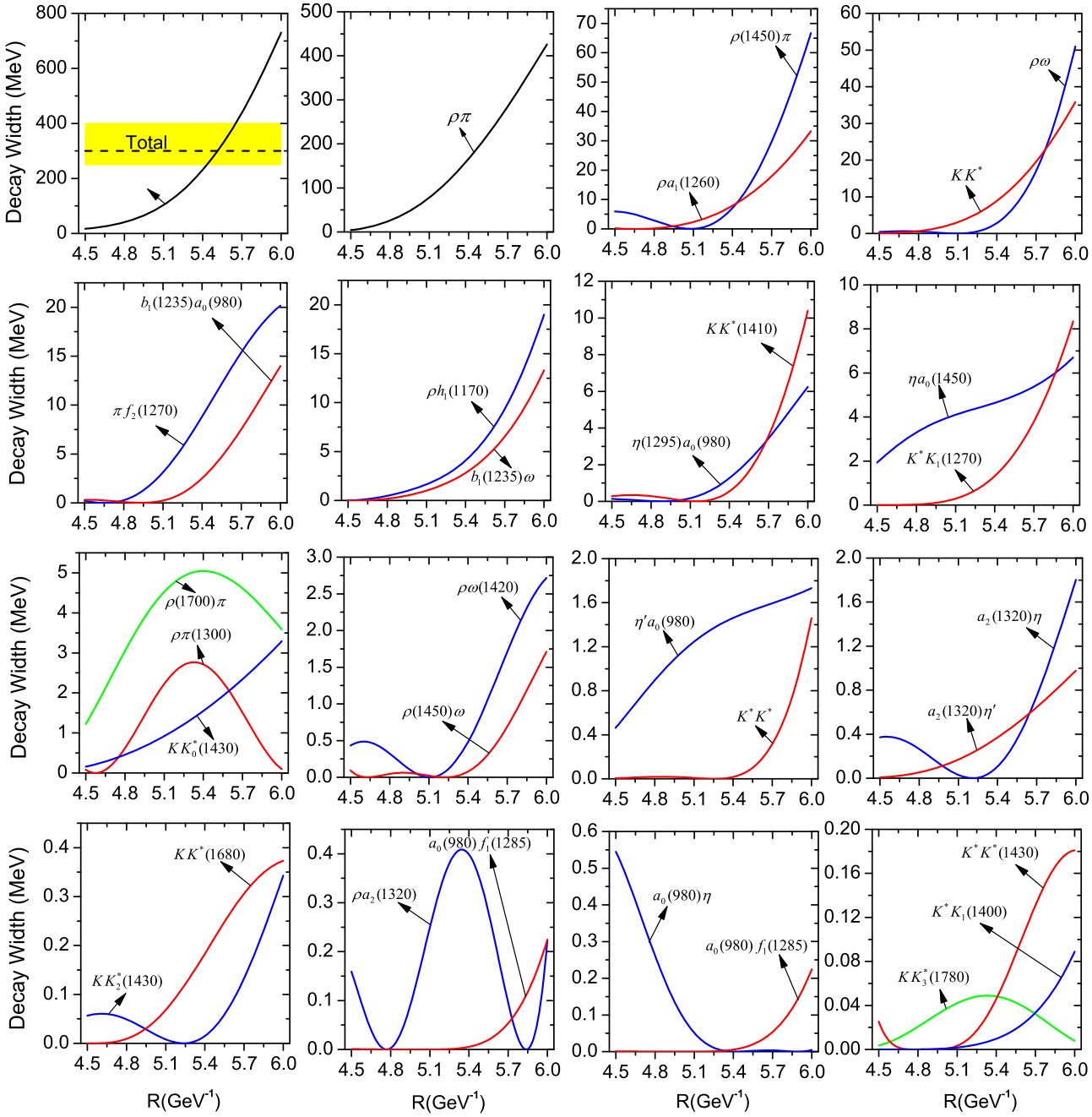

FIG. 7. The R dependence of two-body strong decay widths of $\pi(2360)$ as a $\pi(5S)$ state. The experimental data are marked by the yellow band. Some tiny channels are not drawn.

233 MeV. Here, we choose the typical value of R as 5.65 GeV^{-1}, by which the center value of the experimental data can be reproduced. KK^* and $\eta a_0(1450)$ are two other sizable decay modes, with the widths 18.22 and 14.38 MeV, respectively. The partial widths of $\rho(1450)\pi$, $\rho a_1(1260)$, and $\rho\omega$ are very sensitive to the R value due to the node effects.

The R dependence of the decay width of $X(2100)$ is shown in Fig. 4. We cannot conclude whether or not $X(2100)$ is the $\eta(4S)$, since the error of the experimental width is too large. From Fig. 4, we can see that $\pi a_0(1450)$ is the dominant channel. So we suggest further experiments to study the property of $X(2100)$ via a $\pi a_0(1450)$ decay mode. In addition, we also study the strong decay of $\eta(2010)$, $\eta(2100)$, $X(2120)$, and $\eta(2190)$ under the assignment of the third excitation of $\eta(548)$. Our results indicate that $\eta(2010)$, $\eta(2100)$, and $\eta(2190)$ as the 4^1S_0 isoscalar states are unfavored, whereas $X(2120)$ seems plausible as a candidate of the 4^1S_0 isoscalar state.

As mentioned above, $\eta(2225)$ is a good candidate of $\eta'(4S)$. The plots of decay widths as functions of R are shown

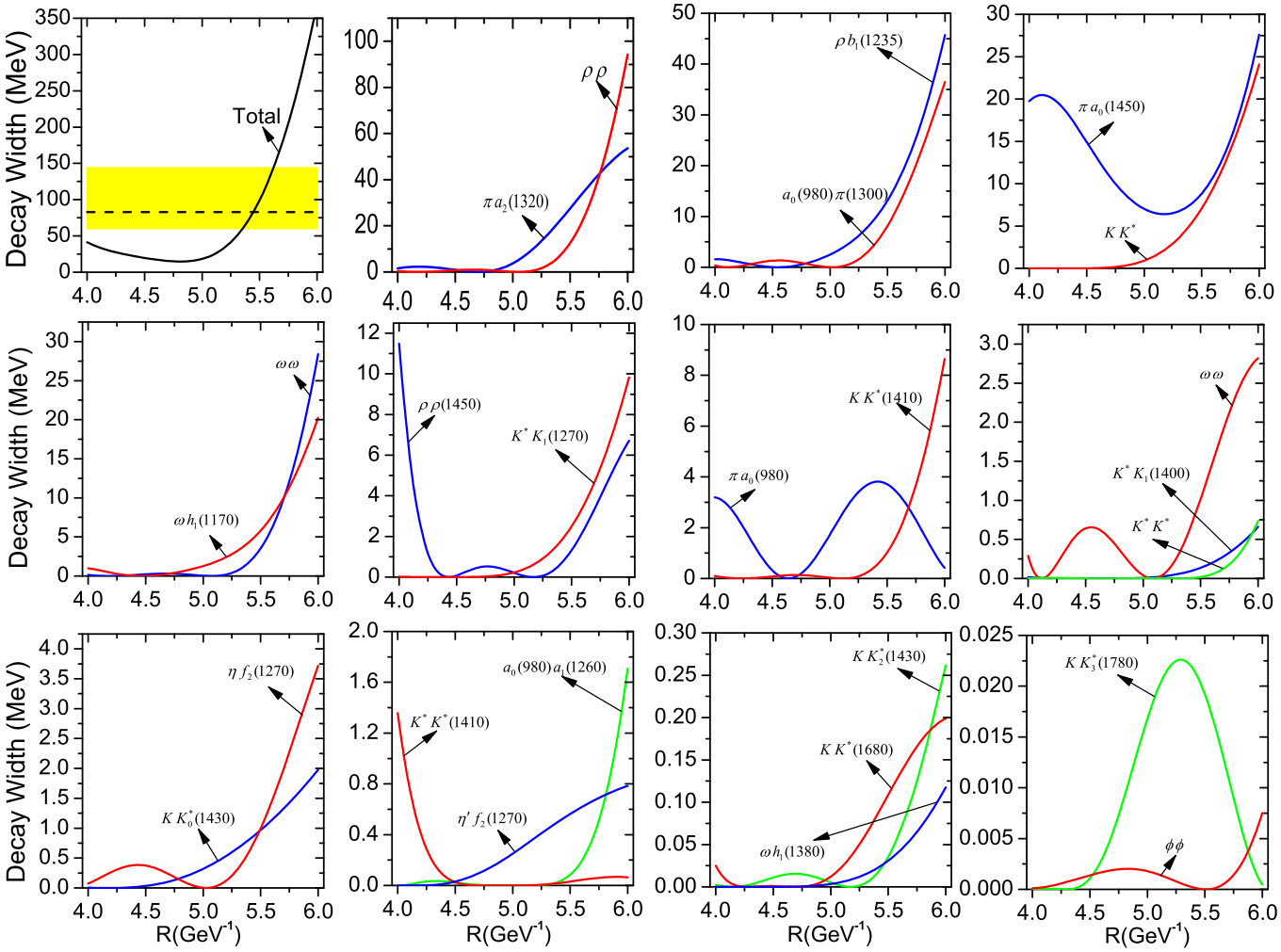

FIG. 8. The R dependence of total decay widths and the partial two-body decay width of $X(2370)$ as the fourth radial excitation of η. The experimental data are marked by the yellow band. Some tiny channels are not drawn. Here, the mixing angle we take is 4.18°.

in Fig. 5. The R value is between 5.01 and 5.32 GeV^{-1}, which gives an overlap of theoretical and experimental data. The plausible range of R agrees with that in Ref. [10]. The main decay channels are KK^* and $KK_0^*(1430)$, which have the partial widths of 147 and 36.67 MeV, respectively. $KK^*(1410)$, $KK_2^*(1430)$, and K^*K^* are highly suppressed due to node effects. The width of the $\phi\phi$ channel is not ignorable, which can naturally explain why $\eta(2225)$ is observed by BES via $J/\psi \to \gamma\phi\phi$ [3].

For $K(2150)$ with 4^1S_0, there is no experimental information at present. Its mass is about 2151 MeV. In Fig. 6, we show the strong decay width of this state, from which we see that the dominant modes are πK^* and ρK. We suggest the experiments to search for $K(2150)$ via these decay channels.

C. Fifth pseudoscalar meson nonet

In the following, we will study the strong decay of the fourth pseudoscalar meson nonet. In Tables II and III, the OZI-allowed decay channels are listed.

$\pi(2360)$ is a good candidate of the 5^1S_0 state. In Fig. 7, we plot the decay width of $\pi(2360)$ depending on R. Comparing to the experimental data, we get the value of R lying in the range $5.43 \sim 5.65$ GeV^{-1}, which is in good agreement with that in Ref. [24]. Its dominant decay channel is $\rho\pi$ with the width 205 MeV. In addition, other channels such as $\rho(1450)\pi$, KK^*, $\rho a_1(1260)$, and $\pi f_2(1270)$ are also important.

The Regge trajectory analysis shows that $X(2370)$ and $\eta(2320)$ can be candidates of the fourth radial excitation of $\eta(548)$. However, our calculation demonstrates that $\eta(2320)$ cannot be $\eta(5S)$ since we cannot reproduce the experimental width of $\eta(2320)$ under this assignment. Under the assignment of $\eta(5S)$, we can get the width of $X(2370)$ which is shown in Fig. 8. If choosing R around 5.44 GeV^{-1} which is similar to Ref. [1], the theoretical value of the total width is equal to the experimental central value. From Fig. 8, we can see that the $\rho\rho$, KK^*, $\pi a_0(1450)$, $a_0(980)\pi(1300)$, $\pi a_2(1320)$, and $\rho b_1(1235)$ channels are important.

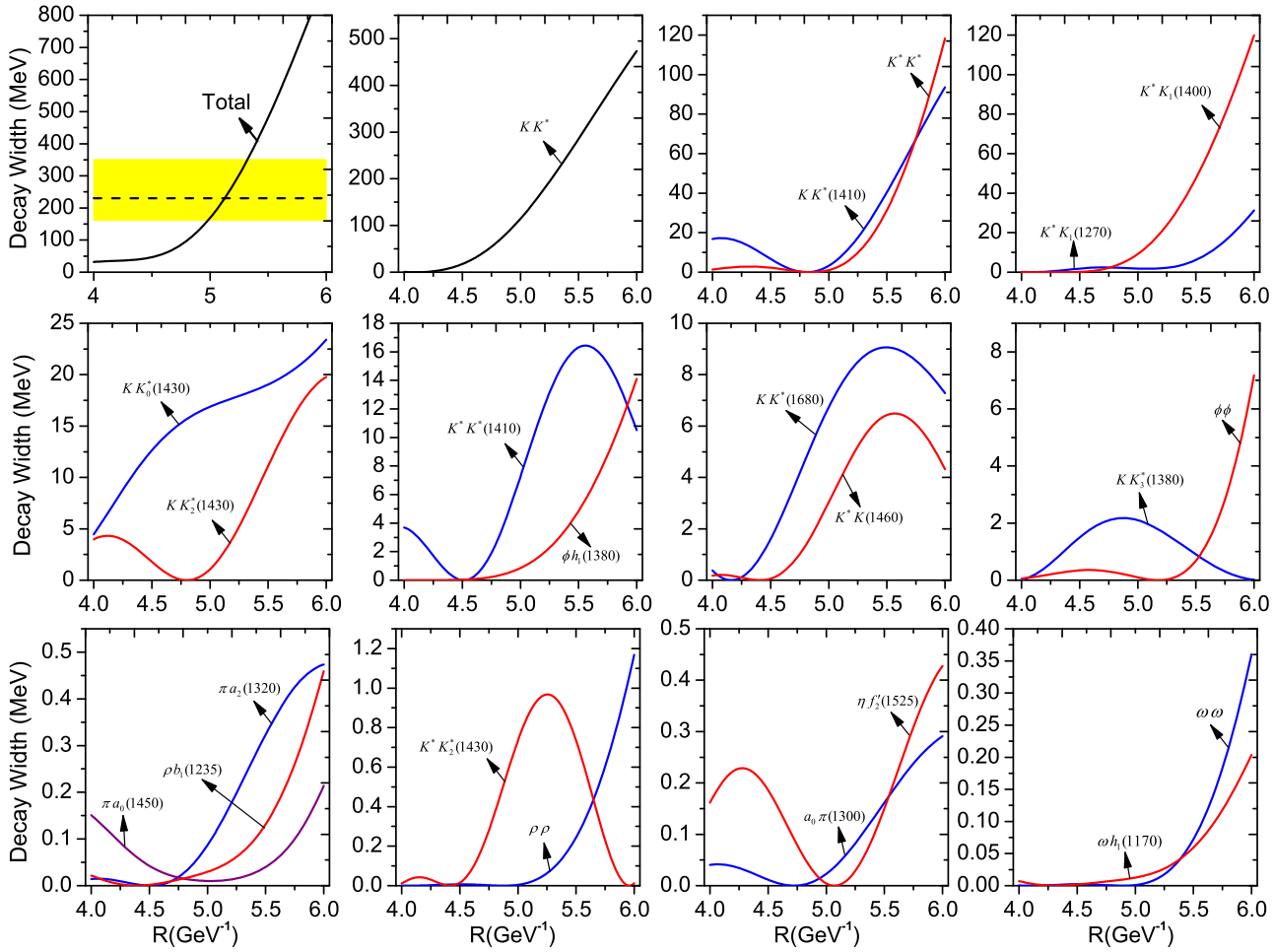

FIG. 9. The R dependence of total decay widths and the partial two-body decay width of $X(2500)$ as the fourth radial excitation of η'. The experimental data are marked by the yellow band. Some tiny channels are not drawn. Here, the mixing angle we take is 4.18°.

According to the mass spectrum analysis, $X(2500)$ is a good candidate of $\eta'(5S)$. In Fig. 9, we plot the decay width of $X(2500)$ under the assignment of the fourth radial excitation of $\eta'(958)$. The value of R corresponding to the central value of the experimental width falls in the range of $4.98 \sim 5.32$ GeV^{-1}. Choosing a typical value of R as 5.13 GeV^{-1}, the dominant decay mode KK^* has the width of 154 MeV. Besides, the $\phi\phi$ channel is not ignorable, which can explain why $X(2500)$ is observed in the $\phi\phi$ channel.

As mentioned in Sec. III, the 5^1S_0 state of the kaon labeled by $K(2414)$ has a mass of 2414 MeV. The strong decay, which is shown in Fig. 10, is dominated by πK^* and ρK. Additionally, $\pi K^*(1410)$, $K\phi$, $K\omega$, and $a_0(980)K$ are also important. This results will be helpful to explore $K(2414)$ in experiment.

V. CONCLUSIONS AND DISCUSSION

Inspired by the observed $X(2100)$, $X(2500)$, and $\eta(2225)$, we have tried to construct new pseudoscalar meson nonets including these states. π, K, $\eta(548)$, and $\eta'(958)$ belong to the ground state pseudoscalar nonet. As stated in Ref. [49], $\pi(1300)$, $K(1460)$, $\eta(1295)$, and $\eta(1475)$ form the first radial excitation of the 0^- meson nonet. The $\pi(1800)$, $K(1830)$, $\eta(1760)$, and $X(1835)$ are grouped into the third pseudoscalar nonet. In this paper, we have speculated that the fourth and fifth pseudoscalar meson nonets are made by $\{\pi(2070), K(2150), \eta(4S), \eta(2225)\}$ and $\{\pi(2360), K(2414), \eta(5S), \eta(2500)\}$, respectively. Here, the candidates for $\eta(4S)$ could be $\eta(2010)$, $\eta(2100)$, $\eta(2190)$, $X(2120)$, and $X(2100)$, while $\eta(5S)$ could be either $X(2370)$ or $\eta(2320)$. Note that $K(2414)$ and $K(2150)$ are predicted particles by using diagonalization of the mass squared matrix and the Gell-Mann-Okubo mass formula. Our speculation has satisfied the Regge trajectories.

Within this scheme, the strong decay of these states has been studied by the flux-tube model. $X(2100)$ or $\eta(2100)$ as a 4^1S_0 state is undetermined since the experimental information is not sufficient. The suggested channel of these two states for further experimental studies is

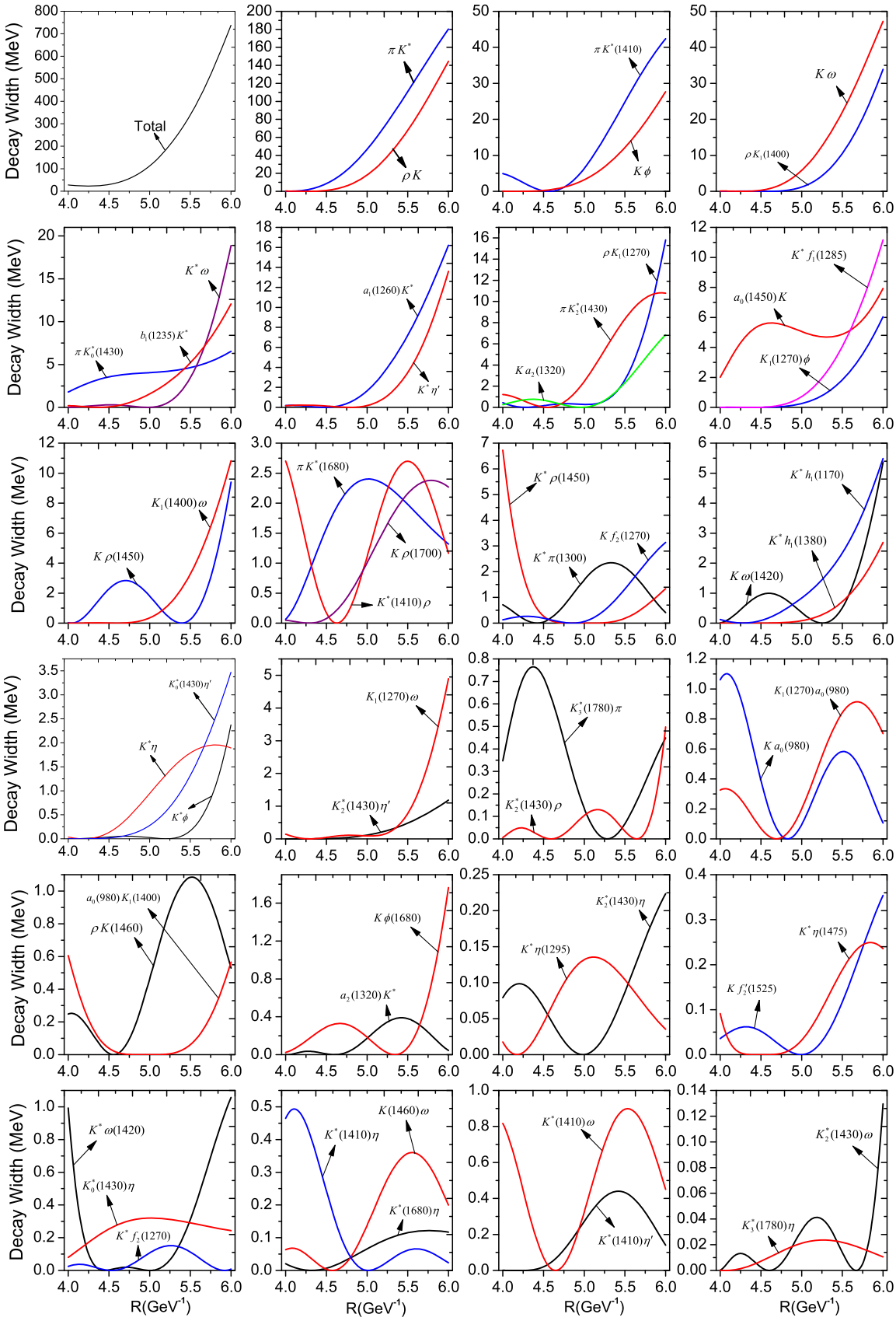

FIG. 10. The R dependence of two-body decay widths of $K(2414)$ as the fourth radial excitation of K. Some tiny channels are not drawn here.

TABLE IV. The pseudoscalar nonets predicted in this paper.

$1S$	$2S$	$3S$	$4S$	$5S$
η,	$\eta(1295)$	$\eta(1760)$	$X(2120)/\eta(2100)/X(2100)$	$X(2370)$
η'	$\eta(1475)$	$X(1835)$	$\eta(2225)$	$X(2500)$
K	$K(1460)$	$K(1830)$	$K(2150)$	$K(2414)$
π	$\pi(1300)$	$\pi(1800)$	$\pi(2070)$	$\pi(2360)$

$\pi a_0(1450)$. We exclude $\eta(2010)$ and $\eta(2190)$ to be the third radial excitation of $\eta(548)$. $X(2120)$ is a good candidate of $\eta(4S)$, which agrees with the conclusion in Ref. [1]. In addition, $\pi(2070)$ and $\eta(2225)$ can be explained as $\pi(4S)$ and $\eta'(4S)$. The predicted particle $K(2150)$ is a candidate for $K(4S)$, the dominant channels πK^* and ρK of which can be tested in future experiments.

Comparing the theoretical and experimental widths, we find that the candidate for $\eta(5S)$ cannot be $\eta(2320)$ but $X(2370)$. The newly observed $X(2500)$ can be interpreted as $\eta'(5S)$. Moreover, we have studied the strong decay of $\pi(2360)$ assuming the quantum number is 5^1S_0, where the calculated width agrees with the experimental one with R around 5.51 GeV^{-1}. The predicted strange meson $K(2414)$ with quantum number 5^1S_0 has been also studied. The total width is in the range of $112.1 \sim 371.8$ MeV with R in the range of 5.0–5.55 GeV^{-1}. We have suggested a further experimental search for this state via πK^* and ρK channels. We have summarized the arrangement of the mesons in Table IV.

The important information of pseudoscalar states provided by BESIII greatly enriches our knowledge on the light hadron spectra. Further experimental and theoretical efforts will be helpful in establishing new pseudoscalar meson nonets. The predicted behaviors of the discussed states can be tested in the near future, and we would like to have more experimental progress of BESIII and the forthcoming BelleII.

ACKNOWLEDGMENTS

We would like to thank the anonymous referee for his suggestions and comments. This work is supported in part by National Natural Science Foundation of China under the Grants No. 11222547 and No. 11175073 and the Fundamental Research Funds for the Central Universities. Xiang Liu is also supported by the National Program for Support of Top-Notch Young Professionals.

[1] J. S. Yu, Z. F. Sun, X. Liu, and Q. Zhao, Categorizing resonances $X(1835)$, $X(2120)$ and $X(2370)$ in the pseudoscalar meson family, Phys. Rev. D **83**, 114007 (2011).
[2] M. Ablikim *et al.* (BESIII Collaboration), Observation of pseudoscalar and tensor resonances in $J/\psi \to \gamma\phi\phi$, Phys. Rev. D **93**, 112011 (2016).
[3] M. Ablikim *et al.* (BES Collaboration), Partial wave analysis of $J/\psi \to \gamma\phi\phi$, Phys. Lett. B **662**, 330 (2008).
[4] A. V. Anisovich, C. A. Baker, C. J. Batty, D. V. Bugg, C. Hodd, H. C. Lu, V. A. Nikonov, A. V. Sarantsev, V. V. Sarantsev, and B. S. Zou, $I = 0$ $C = +1$ mesons from 1920 to 2410 MeV, Phys. Lett. B **491**, 47 (2000).
[5] D. Bisello *et al.* (DM2 Collaboration), First observation of three pseudoscalar states in the $J/\psi \to \gamma\rho\rho$ decay, Phys. Rev. D **39**, 701 (1989).
[6] M. Ablikim *et al.* (BESIII Collaboration), Confirmation of the $X(1835)$ and Observation of the Resonances $X(2120)$ and $X(2370)$ in $J/\psi \to \gamma\pi^+\pi^-\eta'$, Phys. Rev. Lett. **106**, 072002 (2011).
[7] D. M. Li and S. Zhou, Towards the assignment for the 4^1S_0 meson nonet, Phys. Rev. D **78**, 054013 (2008).
[8] J. F. Liu, G.-J. Ding, and M.-L. Yan (BES Collaboration), $X(1835)$ and the new resonances $X(2120)$ and $X(2370)$ observed by the BES collaboration, Phys. Rev. D **82**, 074026 (2010).
[9] Z. G. Wang, Analysis of the $X(1835)$ and related baryonium states with Bethe-Salpeter equation, Eur. Phys. J. A **47**, 71 (2011).
[10] S. Chen and J. Ping, Radial excitation states of η and η' the chiral quark model, Chin. Phys. C **36**, 681 (2012).
[11] T. T. Pan, Q. F. L, E. Wang, and D. M. Li, Strong decays of the $X(2500)$ newly observed by the BESIII Collaboration, Phys. Rev. D **94**, 054030 (2016).
[12] C. R. Deng, J. L. Ping, and F. Wang, Dynamical study of the light scalar mesons below 1 GeV in a flux-tube model, Chin. Phys. C **37**, 033101 (2013).
[13] D. V. Bugg, L. Y. Dong, and B. S. Zou, The broad $J^P = 0^-$ meson in J/ψ radiative decays, Phys. Lett. B **458**, 511 (1999).
[14] C. Patrignani *et al.* (Particle Data Group Collaboration), Review of particle physics, Chin. Phys. C **40**, 100001 (2016).
[15] A. V. Anisovich, V. V. Anisovich, V. N. Markov, M. A. Matveev, V. A. Nikonov, and A. V. Sarantsev, Radiative decays of quarkonium states, momentum operator expansion and nilpotent operators, J. Phys. G **31**, 1537 (2005).
[16] D. M. Li and B. Ma, $\eta(2225)$ observed by BES Collaboration, Phys. Rev. D **77**, 094021 (2008).
[17] A. V. Anisovich, C. A. Baker, C. J. Batty, D. V. Bugg, V. A. Nikonov, A. V. Sarantsev, V. V. Sarantsev, and B. S. Zou, A study of $\rho\rho \to \eta\eta\eta$ for masses 1960 to 2410 MeV, arXiv:1109.4008.

[18] L. S. Geng, R. Molina, and E. Oset, On the chiral covariant approach to $\rho\rho$ scattering, arXiv:1612.07871.
[19] A. Windisch, The analytic properties of the quark propagator from an effective infrared interaction model, Phys. Rev. C **95**, 045204 (2017).
[20] K. Higashijima, Solutions of the spinor-spinor Bethe-Salpeter equation in the scalar-vector sector, Prog. Theor. Phys. **55**, 1591 (1976).
[21] P. Falkensteiner, Matrix elements and decays of baryons in a Bethe-Salpeter model with strong binding, Acta Phys. Austriaca **53**, 175 (1981).
[22] Y. Tomozawa, Normalization of the three-body Bethe-Salpeter wave function for protons, J. Math. Phys. (N.Y.) **24**, 369 (1983).
[23] A. V. Anisovich, C. A. Baker, C. J. Batty, D. V. Bugg, V. A. Nikonov, A. V. Sarantsev, V. V. Sarantsev, and B. S. Zou, A partial wave analysis of $\bar{P}P \to \eta\eta\pi^0$, Phys. Lett. B **517**, 273 (2001).
[24] V. V. Anisovich, L. G. Dakhno, M. A. Matveev, V. A. Nikonov, and A. V. Sarantsev, Quark-antiquark states and their radiative transitions in terms of the spectral integral equation. III. Light mesons, Phys. Atom. Nucl. **70**, 450 (2007); [Yad. Fiz. **70**, 480 (2007)].
[25] D. M. Li and B. Ma, $X(1835)$ and $\eta(1760)$ observed by BES Collaboration, Phys. Rev. D **77**, 074004 (2008).
[26] T. Huang and S. L. Zhu, $X(1835)$: A Natural candidate of eta-prime's second radial excitation, Phys. Rev. D **73**, 014023 (2006).
[27] G. F. Chew and S. C. Frautschi, Regge Trajectories and the Principle of Maximum Strength for Strong Interactions, Phys. Rev. Lett. **8**, 41 (1962).
[28] V. N. Kovalenko, A. M. Puchkov, V. V. Vechernin, and D. V. Diatchenko, Restrictions on pp scattering amplitude imposed by first diffraction minimum data obtained by TOTEM at LHC, arXiv:1506.04442.
[29] P. R. Page, Excited charmonium decays by flux tube breaking and the psi-prime anomaly at CDF, Nucl. Phys. **B446**, 189 (1995).
[30] S. Capstick and N. Isgur, Baryons in a relativized quark model with chromodynamics, Phys. Rev. D **34**, 2809 (1986); AIP Conf. Proc. **132**, 267 (1985).
[31] S. Capstick and W. Roberts, Quasi two-body decays of nonstrange baryons, Phys. Rev. D **49**, 4570 (1994).
[32] E. S. Ackleh, T. Barnes, and E. S. Swanson, On the mechanism of open flavor strong decays, Phys. Rev. D **54**, 6811 (1996).
[33] A. V. Anisovich, V. V. Anisovich, and A. V. Sarantsev, Systematics of $q\bar{q}$ states in the (n, M^2) and (J, M^2) planes, Phys. Rev. D **62**, 051502 (2000).
[34] S. Shu, A practical method in calculating one loop quantum fluctuations to the energy of the non-topological soliton, Sci. China Phys. Mech. Astron. **60**, 041021 (2017)..
[35] K. Golec-Biernat, S. Jadach, W. Placzek, and M. Skrzypek, Solving QCD evolution equations in rapidity space with Markovian Monte Carlo, Acta Phys. Pol. B **39**, 115 (2008); Acta Phys. Pol. A **40**, 213 (2009).
[36] N. V. Krasnikov and A. A. Pivovarov, The use of finite energy sum rules for the description of resonances in QCD, Phys. Lett. **112B**, 397 (1982); Yad. Fiz. **35**, 1270 (1982) [Sov. J. Nucl. Phys. **35**, 744 (1982)].
[37] S. G. Gorishnii, A. L. Kataev, and S. A. Larin, Next Next-to-leading Perturbative QCD Corrections and Light Quark Masses, Phys. Lett. **135B**, 457 (1984).
[38] H. Hatanaka and K. C. Yang, $B \to K_1\gamma$ decays in the light-cone QCD sum rules, Phys. Rev. D **77**, 094023 (2008); Erratum, Phys. Rev. D **78**, 059902(E) (2008).
[39] N. Isgur and J. E. Paton, A Flux Tube Model for Hadrons in QCD, Phys. Rev. D **31**, 2910 (1985).
[40] H. G. Blundell, Meson Properties in the Quark Model: A Look at Some Outstanding Problems, arXiv:hep-ph/9608473.
[41] H. M. Zhao, Z. Q. Zeng, P. N. Shen, Y. B. Ding, and X. Q. Li, Possibly stable configurations of Θ+5 in the flux-tube model, arXiv:nucl-th/0504053.
[42] P. Geiger and E. S. Swanson, Distinguishing among strong decay models, Phys. Rev. D **50**, 6855 (1994).
[43] D. M. Li and S. Zhou, Nature of the $\pi_2(1880)$, Phys. Rev. D **79**, 014014 (2009).
[44] R. Kokoski and N. Isgur, Meson decays by flux-tube breaking, Phys. Rev. D **35**, 907 (1987).
[45] F. E. Close and E. S. Swanson, Dynamics and decay of heavy-light hadrons, Phys. Rev. D **72**, 094004 (2005).
[46] Q. T. Song, D. Y. Chen, X. Liu, and T. Matsuki, Charmed-strange mesons revisited: mass spectra and strong decays, Phys. Rev. D **91**, 054031 (2015).
[47] S. Godfrey and I. T. Jardine, Nature of the $D^*_{s1}(2710)$ and $D^*_{sJ}(2860)$ mesons, Phys. Rev. D **89**, 074023 (2014).
[48] S. Godfrey and N. Isgur, Mesons in a relativized quark model with chromodynamics, Phys. Rev. D **32**, 189 (1985).
[49] E. Klempt and A. Zaitsev, Glueballs, Hybrids, Multiquarks. Experimental facts versus QCD inspired concepts, Phys. Rep. **454**, 1 (2007).